PERGAMON

International Journal of Solids and Structures 37 (2000) 2151–2166

INTERNATIONAL JOURNAL OF SOLIDS and STRUCTURES

www.elsevier.com/locate/ijsolstr

Growth of interfacial cracks in a TBC/superalloy system due to oxide volume induced internal pressure and thermal loading

S.Q. Nusier, G.M. Newaz*

Mechanical Engineering Department, Wayne State University, Detroit, MI 48202, USA

Received 20 September 1997; in revised form 5 November 1998

Abstract

Residual stresses develop in thermal barrier coating during cool down from processing temperature due to the thermal expansion mismatch between the different layers e.g., substrate, bond coat, thermally grown oxide, and TBC. These residual stresses can initiate microcracks at the bond coat/TGO/TBC interfaces and can lead to debonding at the bond coat/TGO/TBC interfaces. Crack like flaws at the interface can be responsible for initiating debonding and accelerating the oxidation process. Effect of oxidation growth between bond coat and ceramic layer (TBC) can be modeled as volume increase. In this part of the investigation, we represent this change in volume as an induced pressure across the crack faces. The energy release rate G, for both Mode I and Mode II cases were evaluated using the virtual crack extension method. The specimen was cooled down from processing temperature of 1025–25°C. The variation of the properties as a function of temperature were used for analysis. A four layer model which includes the TGO layer was analyzed using the finite element method, two cases were considered. Case one is a specimen with a crack at middle of the oxide layer (TGO) while case 2 is a specimen with an interface crack between bond coat and TGO layers. Also, for both cases, a sensitivity study for the effect of variation of materials properties (±25%) was undertaken using the finite element method.

1. Introduction

Thermal barrier coatings (TBCs) are used to sustain the highest temperature at the surface in high temperature super alloy substrates. Plasma-sprayed zirconia-yttria ceramic layer with a nickel-chromium-aluminum-yttrium bond coat on a substrate made of nickel-based superalloy (Chang et al., 1987) is a common superalloy/TBC system. Application of these superalloy/TBC systems can be found

* Corresponding author. Tel.: +1-313-577-3843; fax: +1-313-577-8789.
E-mail address: gnawaz@hub.eng.wayne.edu (G.M. Newaz)

0020-7683/00/$ - see front matter
PII: S0020-7683(98)00321-7

in both aerospace and land-based gas turbine engines. In automotive applications, the piston head for diesel engine is coated to achieve longer life time and higher performance in terms of fuel reduction and power. However, these coatings have durability problems, due to the material and thermal mismatch between the coating and the metallic substrate. Thermal residual stresses develop during cool down from processing temperatures in TBC/metallic substrate. Environmental effects, specifically oxidation, create additional residual stresses due to the growth of an oxide layer causing additional material mismatch between the oxide surface and the TBC. These residual stresses may initiate microcracks such as debonding and radial cracks and can have profound effects on the response of the TBC and interfacial damage accumulation and failure. Their understanding is essential to predict the behavior of the coatings and their performance. The processing technique itself may produce voids or elongated flaws such as air bubbles along the interfaces, which may initiate debonding.

In experimental evaluations conducted in our laboratory for thermal cycling between 200 and 1135°C of nickel based superalloy coated with TBC (Rene' N5 substrate coated with PtAl bond coat and

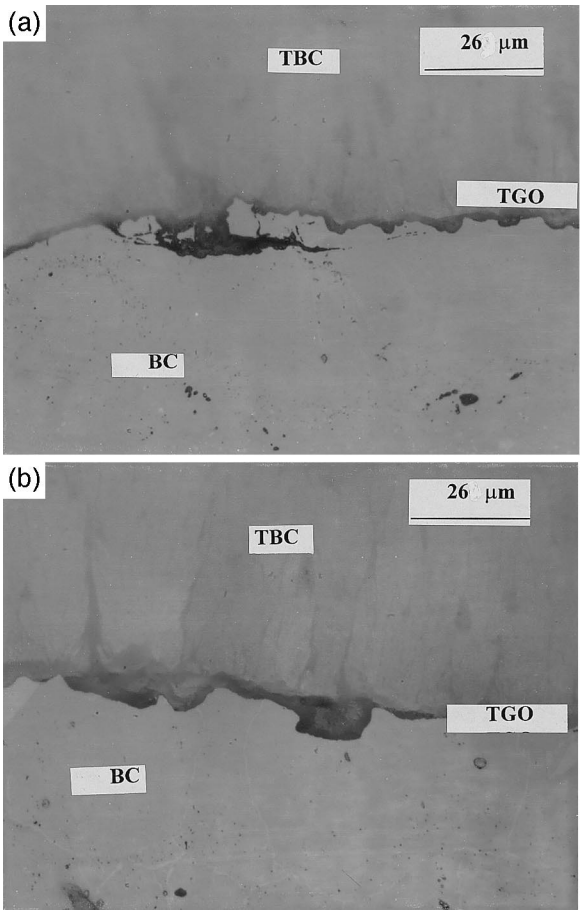

Fig. 1. (a) Interfacial crack at TBC/bond coat interface due to thermal cycling at 200–1135°C in Rene' N5/PtAl/partially stabilized zirconia (2 cycles). (b) Interfacial crack at TBC/bond coat interface due to thermal cycling at 200–1135°C in Rene' N5/PtAl/partially stabilized zirconia (25 cycles).

partially yittria stabilized zirconia TBC), interfacial cracks are found to occur between the TBC and the bond coat as shown in Fig. 1a and b. The mechanics of growth of these cracks under thermal loading is not well known in TBC systems. The current investigation focuses on the nature of crack growth at the bimaterial interface and what are the driving conditions for these cracks under thermo-mechanical loading.

An experimental method and finite element approach was used by Holmes et al. (1988) to study thermal fatigue of coated superalloys of a stepped-disk specimen. The results obtained for the various stress–strain histories clearly illustrate that both the compressive strains encountered on specimen heatup and the tensile strains encountered on cooldown can have a profound effect on useful coating life. An elastic-plastic finite element method was formulated to study residual stresses developed at graded ceramic-metal interfaces during cool down by Williamson et al. (1993). The results demonstrate the importance of accounting for plasticity when comparing graded and nongraded interfaces. They studied the effects of different interlayer thicknesses and nonlinear composition profiles on strain and stress distributions established during cool down (Williamson et al., 1993).

Thermal fracture of multilayer ceramic thermal barrier coatings was studied by Takeuchi and Kokini (1994). Controlled experiments along with finite element modeling were used. Their work showed that surface cracks are formed as a result of tensile stresses that are created following stress relaxation in the TBC at steady-state high temperatures. The effect of a transient thermal load on a coating which is bonded to a cylindrical substrate was studied by Kokini and Hornack (1988). A finite element method was used to obtain a solution for a circumferential edge crack normal to the coating. Their analysis showed that smaller heat transfer rates result in smaller stress intensity factors. The finite element method has been used in conjunction with a numerical interface fracture mechanics model to investigate the structural response of coated brittle materials subjected to normal and shear loads, by Oneil and Wayne (1994). They examined how flaw orientation affects crack propagation through the coating, interface, and substrate. A comparison between the uncoated and coated substrate has shown that cracks are strongly influenced toward interfaces because of the preferred release of critical strain energy. A finite element model to calculate the Mode II stress-intensity factors was developed by Van der Zande and Grootenboer (1986). The optimum size for a so-called singular element has been determined. Suo (1995) studied wrinkles which induce interfacial stresses and cause voiding. A linear bifurcation analysis has been carried out when wrinkles just start. The oxide scale thickens slowly at a higher temperature, until the compressive stress generated by oxidation and cooling causes it to spall off. The strain energy release rate components G_{I} and G_{II} in Mode I and Mode II at the tip of an interface crack in a bimaterial plate under tension in a direction normal to the interface were evaluated using a finite element analysis and modified crack closure integral (MCCI) technique by Dattaguru et al. (1994). The finite element results for all the models show increasing Mode II dominance as the crack tip element becomes finer. An elastoplastic solution for the interface crack with contact zones was studied by Aravas and Sharma (1991). It was shown that the elastic asymptotic solutions based on the assumption of a closed crack tip predicted material interpenetration. Also, it was shown that the asymptotic solution is separable in r and θ at the crack tip. Singular thermal stress fields in bonded viscoelastic quarter planes were studied by Blanchard and Ghoniem (1989). It was shown that the order of the singularity generally increases with time. Singular stress and heat flux fields at the tip of the crack in a general nonhomogeneous material were studied by Jin and Noda (1994). It was found that the crack-tip field singularities and angular distributions are the same as those in the homogeneous material. New domain integrals for axisymmetric interface crack problems are derived by Nahta and Moran (1993). The effect of crack front curvature is shown to play an important role in the derivation of the integrals.

The mechanics of the delamination and spalling of compressed films or coatings has been analyzed using a combination of fracture mechanics and post-buckling theory by Evans and Hutchinson (1984). The phenomenon of delamination buckling and growth in a time dependent radial compressive load was

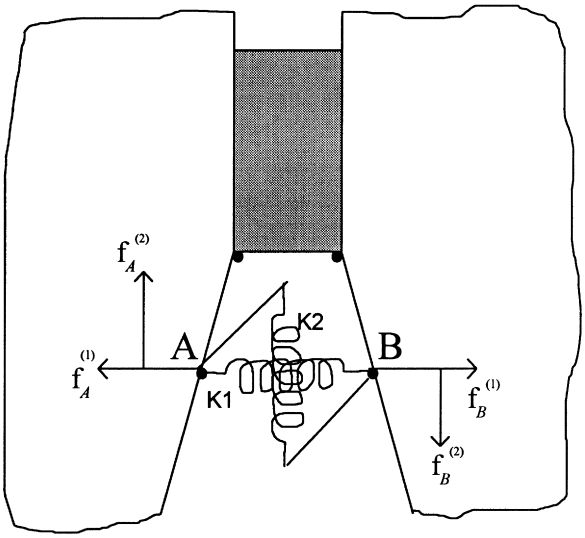

Fig. 2. Forces and displacement illustrations for an interfacial crack.

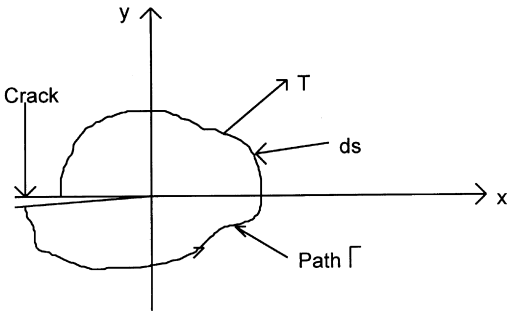

Fig. 3. Notation and parameters used for *J*-integral.

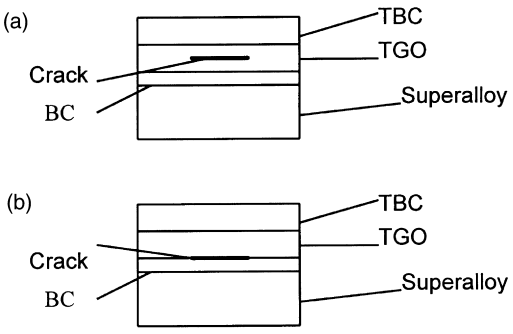

Fig. 4. (a) Circumferential crack at middle of the oxide layer in a stepped-disk specimen. (b) Circumferential crack between the oxide layer and the bond coat layer in a stepped-disk specimen.

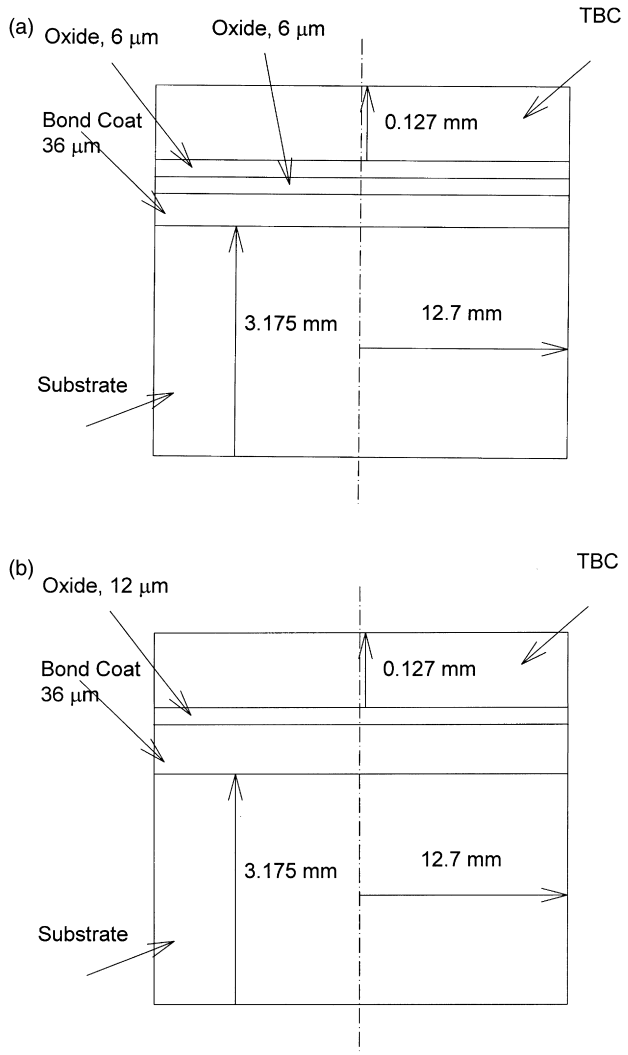

Fig. 5. (a) Dimension of TBC layer in relation to bond coat and superalloy substrate for the case of middle oxide layer crack. (b) Dimension of TBC layer in relation to bond coat and superalloy substrate, for the case of TGO/BC interface crack.

analyzed by Bottega and Maewal (1983a, b). An iterative procedure based on the fourth-order Runge–Kutta integration formula was used to generate a family of nondimensionalized postbuckling solutions of von Karman's nonlinear plate theory by Yin (1985). A mixed-mode fracture analysis combining nonlinear thin-plate stress solutions with crack-tip elasticity results has been developed to account for local variations of G_{I}, G_{II}, and G_{III} in thin-film debond problems associated with large film deformations by Chai (1990). A shaft-loaded blister test has been developed by Wan and Mai (1995) to measure the interfacial energy of a thin flexible polymeric film adhered to a rigid substrate. A theoretical analysis is given of an axisymmetric debond ('blister'). Expressions have been derived which describe the critical stress and pressure necessary to rupture oxide blisters which form on aluminum during growth of corrosion pits by Ryan and McCafferty (1995).

Table 1
Material properties at 22, 566 and 1149°C

Material	Young's modulus (GPa)	Poisson's ratio	Coefficient of thermal expansion ($°C^{-1}$)
Substrate	175.8	0.25	13.91×10^{-6}
	150.4	0.2566	15.36×10^{-6}
	94.1	0.3224	19.52×10^{-6}
Bond coat	137.9	0.27	15.16×10^{-6}
	121.4	0.27	15.37×10^{-6}
	93.8	0.27	17.48×10^{-6}
TBC	27.6	0.25	10.01×10^{-6}
	6.9	0.25	11.01×10^{-6}
	1.84	0.25	12.41×10^{-6}
Oxide	386	0.257	6×10^{-6}
	349	0.257	8×10^{-6}
	311	0.257	8.9×10^{-6}

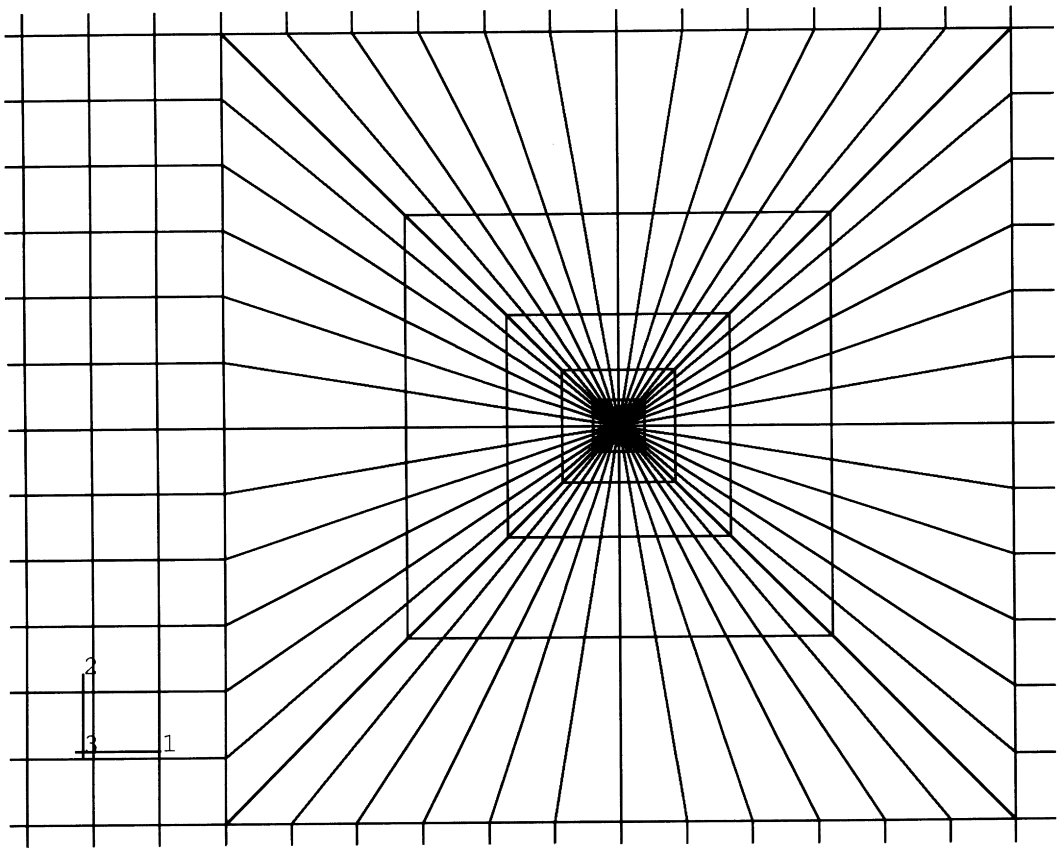

Fig. 6. Details of the finite element mesh near the crack tip.

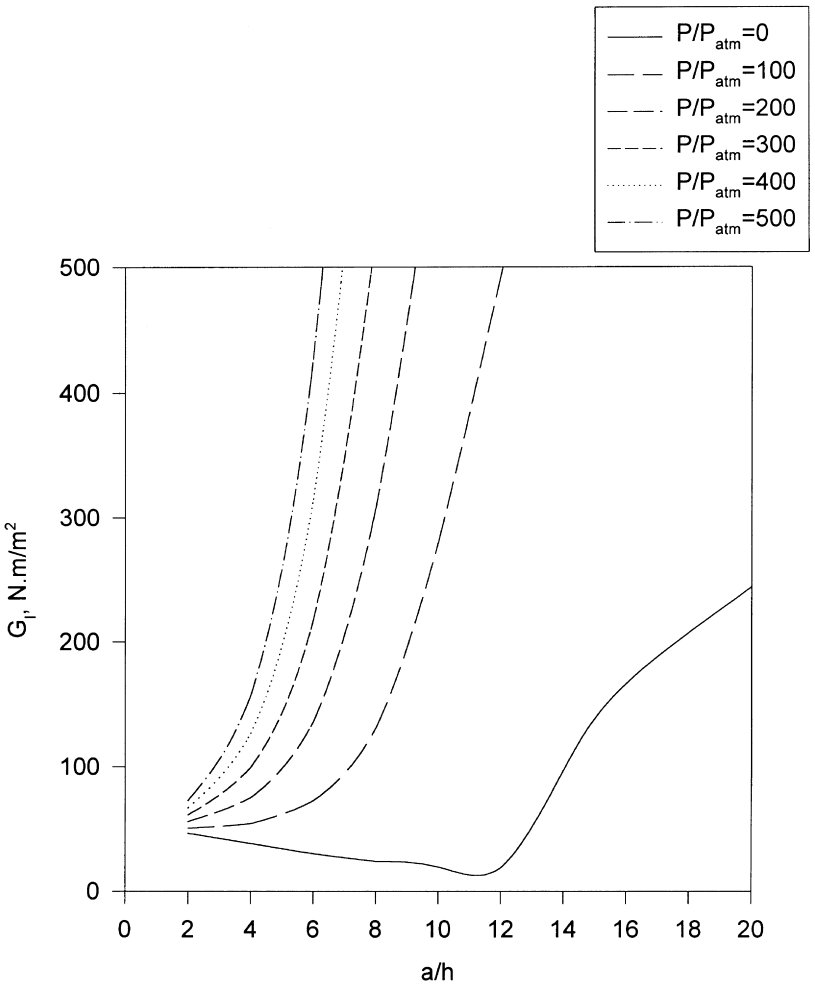

Fig. 7. Variation of G_I versus delamination radius at different pressure ratio (for the case shown in Fig. 4a).

2. Analytical aspects

2.1. Virtual crack extension method (VCEM)

Within linear elastic fracture mechanics, two parameters are generally used to describe the conditions at the crack tip, normally the stress intensity factor and the energy release rate. Evaluation of the stress intensity factor requires a thorough understanding of the state of stress at the crack tip. Energy release rate evaluation, on the other hand, is based more on an energy criteria and is hence more popular.

A procedure for calculating the energy release rate, G, that has gained increasing acceptance over the past decade is the Virtual Crack Extension Method (VCEM). This was originally developed by Hellen (1975), who subsequently extended the method to cover material non-linearities, and the evaluation of the J-integral.

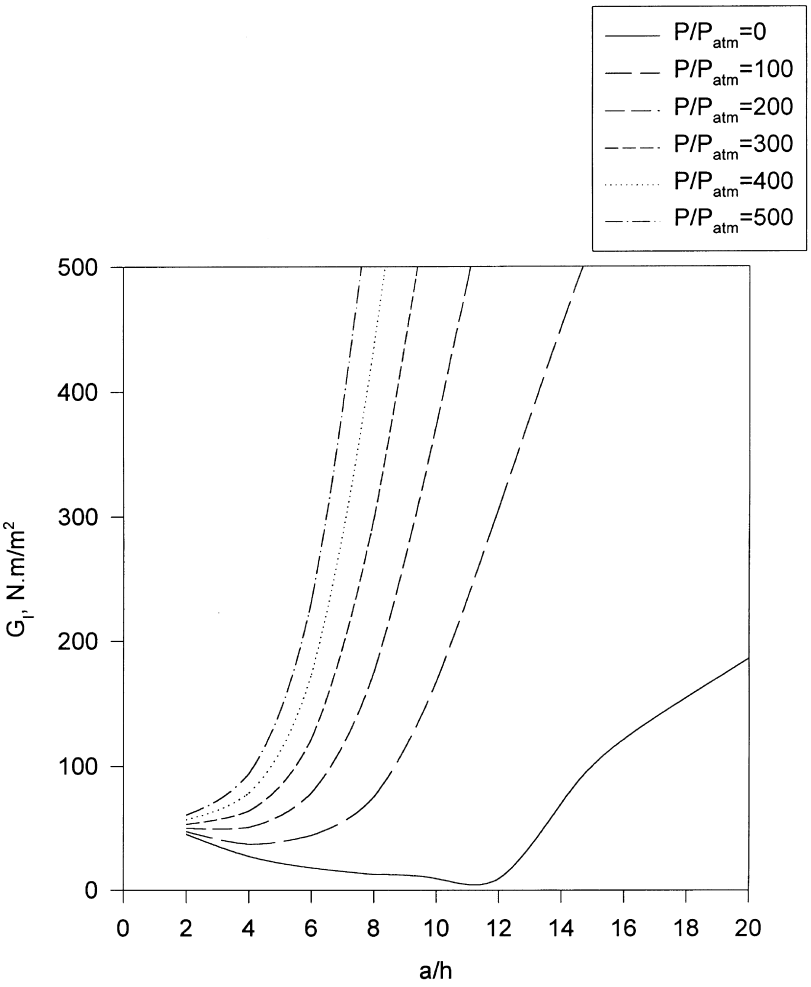

Fig. 8. Variation of G_{I} versus delamination radius at different pressure ratio (for the case shown in Fig. 4b).

The method of VCE used to evaluate G is explained in the following few steps. Consider Fig. 2, the energy release rates in Mode I and II are given by

$$G_{\mathrm{I}} = \frac{1}{2A} f_x \Delta u_x$$

$$G_{\mathrm{II}} = \frac{1}{2A} f_y \Delta u_y \tag{1}$$

where f_x and f_y are the reaction forces, A is the crack surface area corresponding to Δa, and similarly Δu_x and Δu_y are the difference in the displacements of nodes A and B in the x- and y-directions respectively (Fig. 2).

The reaction forces and the displacements are obtained via two runs. For the first run, we assume a

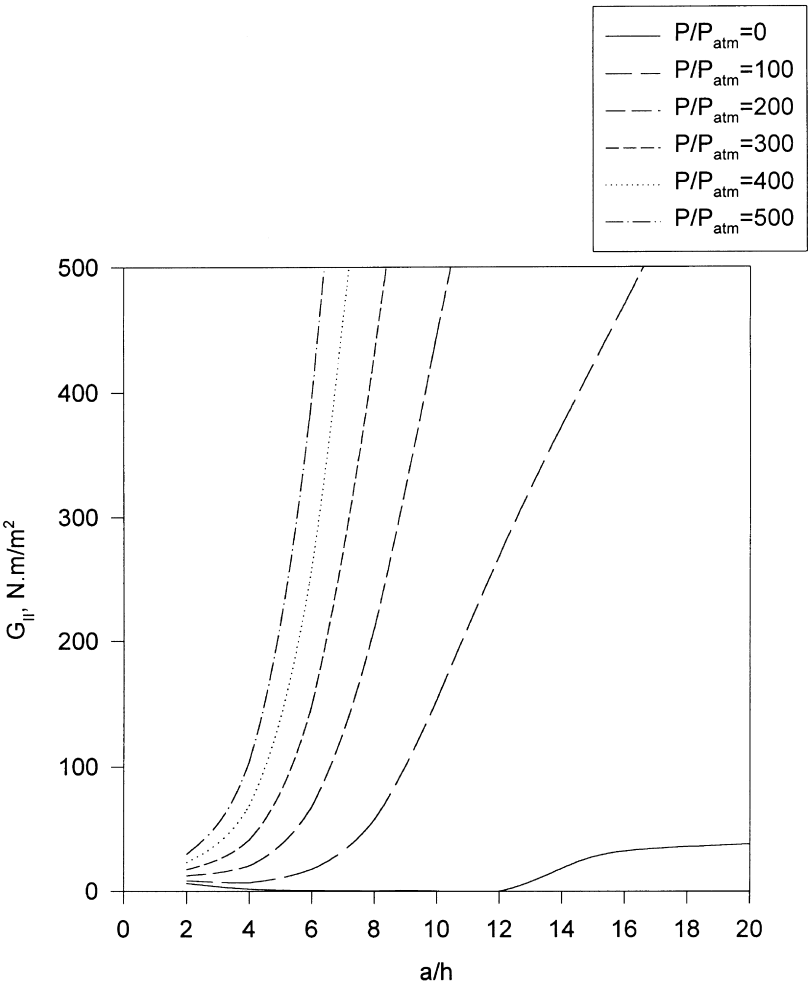

Fig. 9. Variation of G_{II} versus delamination radius at different pressure ratio (for the case shown in Fig. 4a).

very weak spring, so the opening displacement and sliding displacement can be determined from springs deflection. In the second run the spring stiffness is assumed to be very high compared to the material stiffness, so the reaction forces can be determined. In this study an eight node isoparametric element is used, the energy release rates in Mode I and Mode II are given by

$$G_{\mathrm{I}} = \frac{1}{2A}\left[f_{x1}\Delta u_{x1} + f_{x2}\Delta u_{x2}\right]$$

$$G_{\mathrm{II}} = \frac{1}{2A}\left[f_{y1}\Delta u_{y1} + f_{y2}\Delta u_{y2}\right] \tag{2}$$

Hence

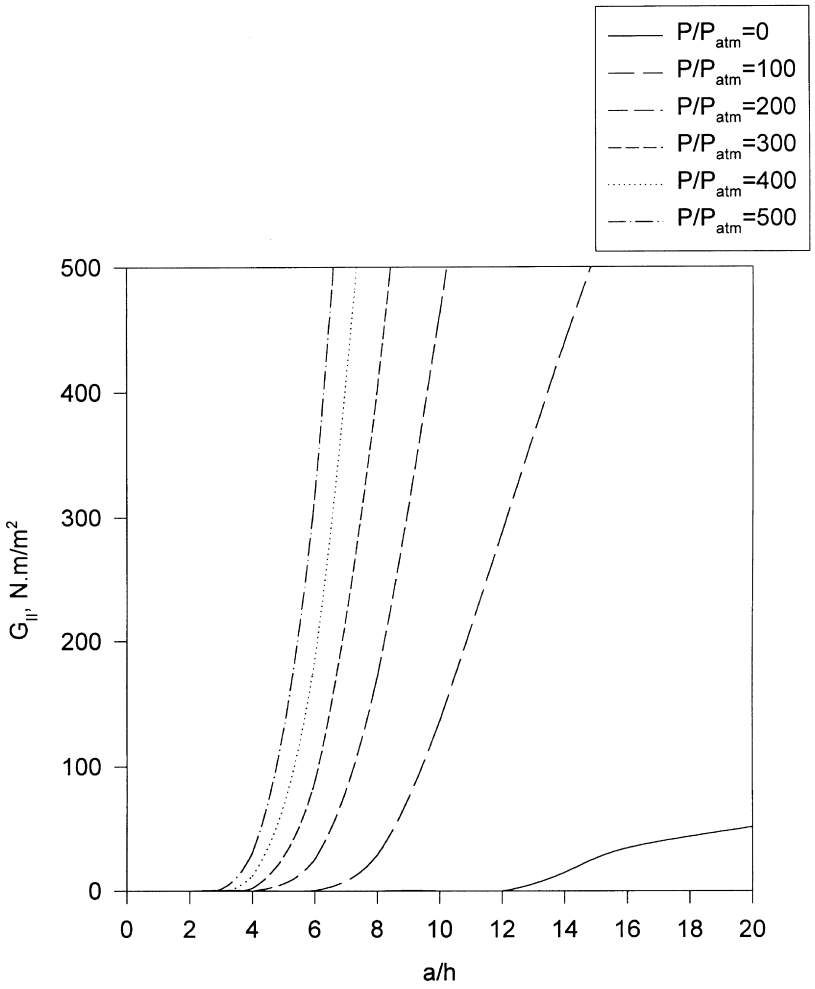

Fig. 10. Variation of G_{II} versus delamination radius at different pressure ratio (for the case shown in Fig. 4b).

$$G_t = G_I + G_{II} \tag{3}$$

Another approach to characterize fracture at bimaterial interface is via the *J*-integral. Originally developed by Eshelby (1956), the basic concept of *J*-integral is a path independent evaluation of the energy release rate. In other words, it is a measure of decrease in potential energy of the system with increase in crack length. In linear elastic fracture mechanics '*J*' is equivalent to *G*. The *J*-integral can be written as (Rice, 1968)

$$J = \int_\Gamma W \, dy - \int_\Gamma T \frac{\partial u}{\partial x} ds \tag{4}$$

where *W* is the strain energy density. Fig. 3 shows the notation and parameters for *J*-integral for a homogeneous medium. The analysis can be easily extended for a line crack between two materials

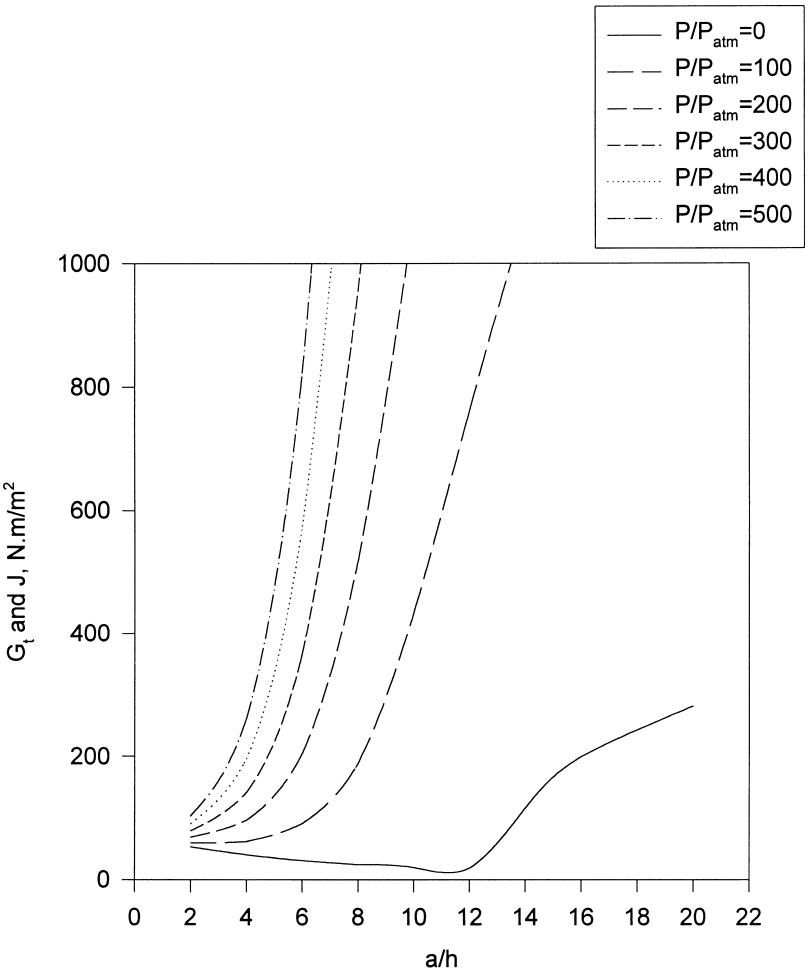

Fig. 11. Variation of G_I and J versus delamination radius at different pressure ratio (for the case shown in Fig. 4a). Note that G_t and J coincide.

assuming crack growth along the interface. The essence of J-definition and its meaning remains unaltered for a crack at the bimaterial interface.

There is one idealized condition that we explored related to the specimen geometry. The presence of circumferential at the middle of the oxide layer, and between the oxide layer and the bond coat layer are shown in Fig. 4a and b which was analyzed using the finite element method. The general code ABAQUS (1995) was used for these analyses. The energy release rate G can be estimated by using the virtual crack extension method. The J-integral value can be found directly from ABAQUS.

3. Results and discussion

The presence of circumferential crack at middle of TGO layer, and at the interface between TGO

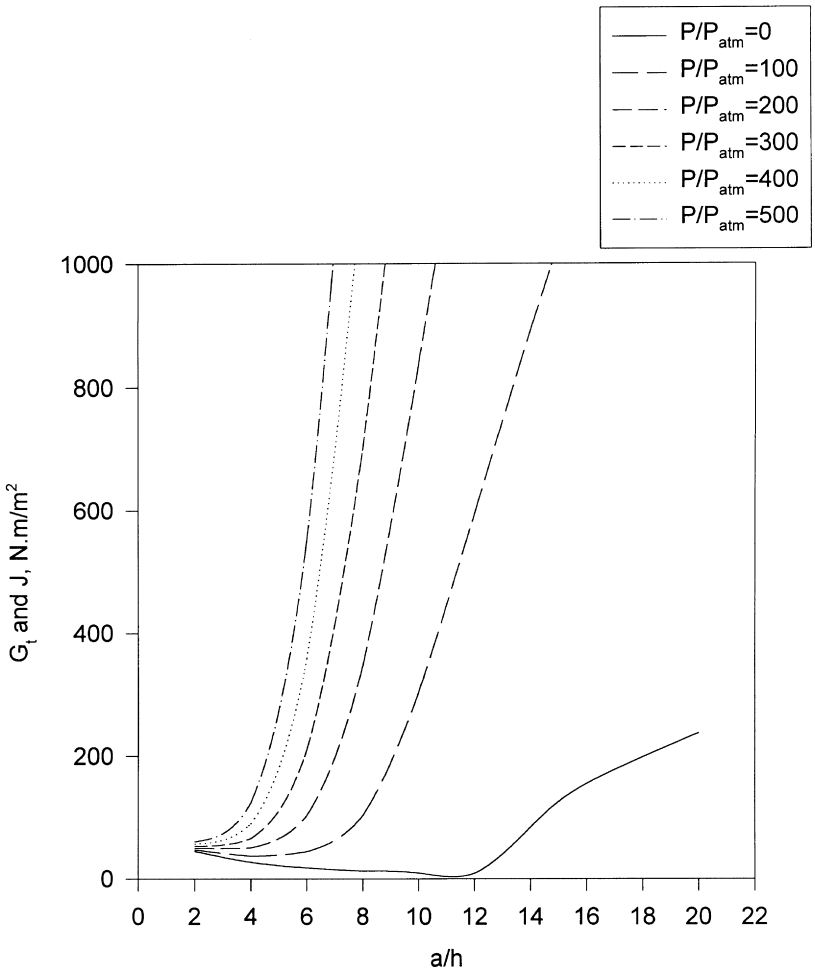

Fig. 12. Variation of G_t and J versus delamination radius at different pressure ratio (for the case shown in Fig. 4b). Note that G_t and J coincide.

layer and bond coat layer as shown in Fig. 4a and b, respectively, was analyzed using the finite element method. The general code ABAQUS was used for finite element analysis. The energy release rate G was estimated by using the virtual crack extension method.

Finite element method was used in order to determine the J-integral value and the energy release rate. Virtual crack extension method was used to evaluate the energy release rate for both Mode I and Mode II crack growth. For stepped-disk specimen, the disk radius is 12.7 mm, the bond coat layer thickness is 0.036 mm, the TGO thickness is 0.012 mm, the TBC thickness is 0.127 mm, and the uncoated nickel based superalloy had a thickness of 3.175 mm. The dimensions of a specimen with a crack at middle of oxide layer is shown in Fig. 5a, while Fig. 5b, shows the dimension of the specimen which has a crack at the oxide/bond coat interface. The properties of these four layers are given in Table 1. We analyzed a model case where the specimen was plasma sprayed in air with a thin zirconia-yttria (ZrO_2–8 wt% Y_2O_3) layer on a nickel-chromium-aluminum-zirconium bond coat (Chang et al., 1987). The specimen was cooled down from a processing temperature of 1025°C to a temperature of 25°C.

Half model for stepped-disk specimen was used since the specimen is axisymmetric. Eight node

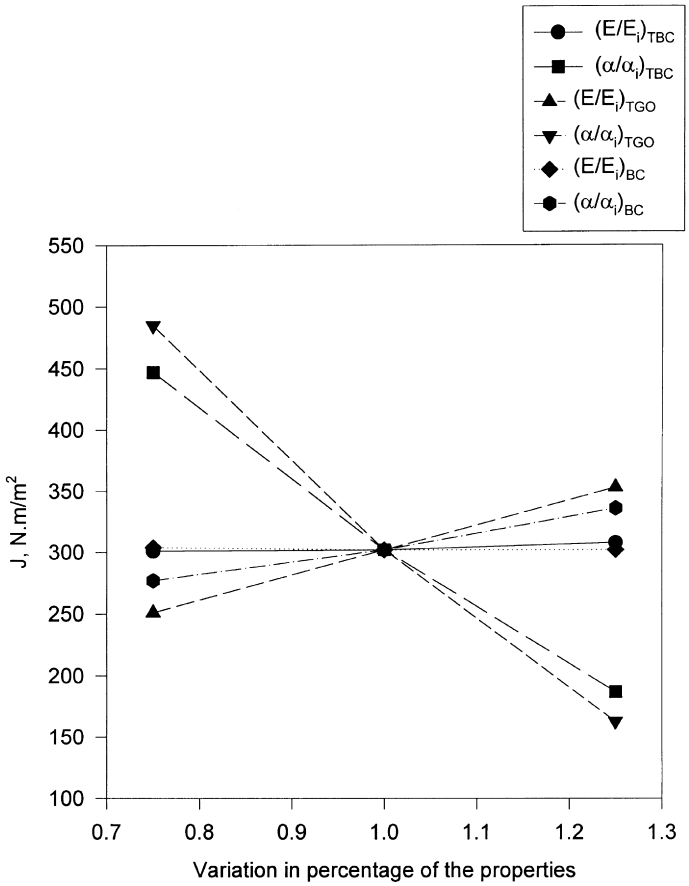

Fig. 13. Variation of J versus variation percentage in properties for a crack located middle of TGO layer.

isoparametric element type was used; the total number of elements was 1380. Along the longitudinal axis, the nodes can move in the axial direction only. The mesh was very fine close to the crack tip, and to make sure that the mesh is fine enough, another model with the same number of element but has one tenth of element size near to the crack tip, the difference in the results was less than 1%. Details of the finite element mesh near the crack tip is shown in Fig. 6. Figs 7–12 show the variation of G_{I}, G_{II}, and G_{t} versus delamination radius at different pressure levels for two different crack locations (Fig. 4a and b), respectively. The conditions for crack propagation can be obtained from these Figures ($G \geq 30$ N/m). It is clear from these Figures that TGO/bond coat interface crack has a lower energy release value in comparison to a crack at middle of oxide layer (note that the values are close to each other). Figs 11 and 12 show the variation of total energy release rate versus delamination radius for both cases (Fig. 4a and b). From these Figures one can obtain the conditions when the crack will propagate. From literature the critical energy release rate is varied between 10 and 30 Nm m^2 for this system configuration. For a value of 30 J/m^2, and a delamination radius of four times the TBC thickness, the crack will propagate at induced pressure value equivalent to 500 atmosphere ($\approx$50 MPa). This value is easy to develop due to volume increase because of oxide layer growth. Also, based on finite element analysis conducted by the authors (Nusier and Newaz, 1998) for this system with a wavy interface, the results shows that an axial stress of 185 MPa can be developed for a sine wave interface with amplitude

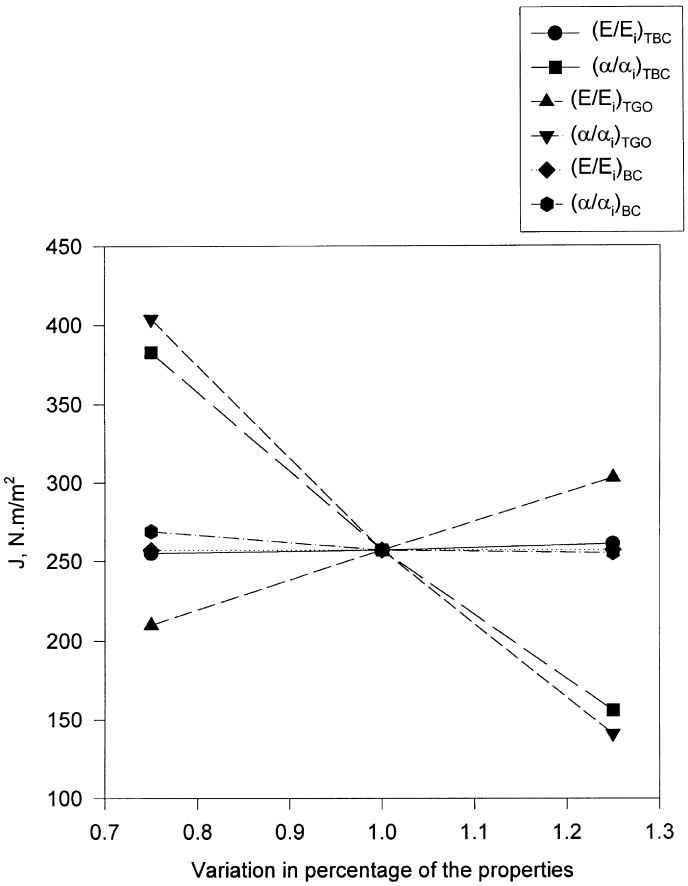

Fig. 14. Variation of J versus variation percentage in properties for a crack located at TGO/BC interface.

of 2.4 μm and wave length of 127 μm. These values are practical for this system (Nusier and Newaz, 1998).

Figs. 13 and 14 show a sensitivity plot for variation effect in properties on the total energy release rate for both cases.

4. Summary and conclusions

The effect of interfacial microcracks was investigated using a fracture mechanics approach under combined internal pressure at crack surface and thermal loading (thermo-mechanical loading). The surface pressure is considered due to volume increase of oxide scales in the TGO layer. Stepped-disk type specimen with a central crack has mixed mode conditions under thermo-mechanical loading. The total energy release rate evaluated by the virtual crack extension method and the J-integral value evaluated directly by ABAQUS agree quite well. For a TGO toughness value of 30 J/m^2, and a delamination radius of four times the TBC thickness, the crack will propagate at induced pressure value equivalent to 500 atmosphere ($\approx$50 MPa). The results clearly indicate that small internal pressure due to oxidation induced volume change may create the necessary conditions for crack growth during thermal

cycling. This value may easily develop due to volume increase because of oxide layer growth or due to the presence of a wavy interface. The value of the energy release rate is very sensitive to thermal expansion coefficient, on the other hand it is less sensitive to variation in modulus of elasticity.

Acknowledgements

Funding for this research was provided through a grant (No. F49620-95-1-0201) from the Air Force Office of Scientific Research (AFOSR). Dr Ozden Ochoa is the program monitor. Discussion and interaction with Dr P.K. Wright of GEAE is gratefully acknowledged.

References

ABAQUS, 1995. Hibbitt, Karlsson and Sorensen, Inc.

Aravas, N., Sharma, S.M., 1991. An elastoplastic analysis of the interface crack with contact zones. J. Mech. Phys. Solids 39 (3), 311–344.

Blanchard, J.P., Ghoniem, N.M., 1989. Relaxation of thermal stress singularities in bonded viscoelastic quarter planes. Transactions of the ASME 56, 756–762.

Bottega, W.J., Maewal, A., 1983a. Delamination buckling and growth in laminates. Transactions of the ASME 50, 184–189.

Bottega, W.J., Maewal, A., 1983b. Dynamics of delamination buckling. International Journal of Non-Linear Mechanics 18 (6), 449–463.

Chai, H., 1990. Three-dimensional fracture analysis of thin-film debonding. Int. J. Fracture 46, 237–256.

Chang, G.C., Phucharoen, W., Miller, R.A., 1987. Finite element thermal stress solutions for thermal barrier coatings. Surface and Coatings Technology 32, 307–325.

Dattaguru, B., Venkatesha, K.S., Ramamurthy, T.S., Buchholz, F.G., 1994. Finite element estimates of strain energy release rate components at the tip of an interface crack under mode I loading. Engineering Fracture Mechanics 49 (3), 451–463.

Eshelby, J.D., 1956. The continuum theory of lattice defects. Solid State Physics 3, 79–141.

Evans, A.G., Hutchinson, J.W., 1984. On the mechanics of delamination and spalling in compressed films. Int. J. Solids Struct 20 (5), 455–466.

Hellen, T.K., 1975. On the method of virtual crack extensions. Int. J. Num. Meth 9, 187–207.

Holmes, J.W., McClintock, F.A., O'Hara, K.S., Conners, M.E., 1988. Thermal fatigue testing of coated monocrystalline superalloys. Low Cycle Fatigue ASTM STP 942, 672–691.

Jin, Z., Noda, N., 1994. Crack-tip singular fields in nonhomogeneous materials. Transactions of the ASME 61, 738–740.

Kokini, K., Hornack, T.R., 1988. Transient thermal load effects on coatings bonded to cylindrical substrates and containing circumferential cracks. Journal of Engineering Materials and Technology 110, 35–40.

Nahta, R., Moran, B., 1993. Domain integrals for axisymmetric interface crack problems. Int. J. Solids Struct 30 (15), 2027–2040.

Newaz, G.M., Nusier, S.Q., Chaudhury, Z.A., 1998. Damage accumulation mechanisms in thermal barrier coatings. ASME, Journal of Engineering Materials and Technology 120 (2), 149–153.

Nusier, S.Q., Newaz, G.M., 1998. Analysis of interfacial cracks in a TBC/superalloy system under thermal loading. Journal of Engineering Fracture Mechanics 60 (5–6), 577–581.

Oneil, D.A., Wayne, S.F., 1994. Numerical simulation of fracture in coated brittle materials subjected to tribo-contact. Journal of Engineering Materials and Technology 116, 471–478.

Rice, J.R., 1968. Mathematical analysis in the mechanics of fracture. In: Leibowitz, H. (Ed.), Fracture, An Advanced Treatise Vol. 2. Academic Press, New York, pp. 191–311.

Ryan, R.L., McCafferty, E., 1995. Rupture of an oxide blister. J. Electrochem. Soc 142 (8), 2594–2597.

Suo, Z., 1995. Wrinkles of the oxide scale on an aluminum-containing alloy at high temperature. Journal of Mechanics and Physics of Solids 43 (6), 829–846.

Takeuchi, Y.R., Kokini, K., 1994. Thermal fracture of multilayer ceramic thermal barrier coatings. Journal of Engineering for Gas Turbines and Power. Trans. ASME 116, 266–271.

Van der Zande, H.D., Grootenboer, H.J., 1986. A finite element approach to interface cracks. Journal of Applied Mechanics 53, 573–578.

Wan, K., Mai, Y., 1995. Fracture mechanics of a shaft-loaded blister of thin flexible membrane on rigid substrate. Int. J. Fract 74, 181–197.

Williamson, R.L., Rabin, B.H., Drake, J.T., 1993. Finite element analysis of thermal residual stresses at graded ceramic-metal interfaces: part I—Model description and geometrical effects. J. Appl. Phys 74, 1310–1320.

Yin, W., 1985. Axisymmetric buckling and growth of a circular delamination in a compresses laminate. Int. J. Solids and Struct 21 (5), 503–514.